Effect of the Metallization on the Resonances of THz Fishnet Metamaterials

C. Sabah
Sabah@Physik.uni-frankfurt.de
Johann Wolfgang Goethe-Universität, Physikalisches Institut, Max-von-Laue-Str. 1, D-60438 Frankfurt am Main, Germany

H. G. Roskos
Johann Wolfgang Goethe-Universität, Physikalisches Institut, Max-von-Laue-Str. 1, D-60438 Frankfurt am Main, Germany

In this numerical study, the influence of the choice of metal (and hence of the conductivity) used for the fabrication of THz fishnet metamaterials is investigated. We explore an exemplary structure for which surface-plasmon-polaritons offer – assuming sufficiently good conductivity – pronounced extraordinary transmission and strong multiple magnetic resonances with negative permeability. We analyze the dependence of these signatures on the type of metallization. Studying five different metals, we find that the metallization is important for achieving the multiple resonances. A reduction of the conductivity can lead to a dramatic weakening and even a near-disappearance of magnetic resonances if they lose their diamagnetic character. [DOI: http://dx.doi.org/10.2971/jeos.2012.12005]

Keywords: Metamaterials, Fishnet Metamaterials, Surface-Plasmon-Polaritons, Negative Permeability, Negative Permittivity, Negative Refractive Index, THz Wave, Multiple Resonances

1 INTRODUCTION

Fishnet metamaterials (MTMs), which consist basically of two holey metal films separated by a dielectric slab, have attracted considerable attention recently because they combine structural simplicity with great versatility. Another advantage is that they typically exhibit lower losses (and a better figure of merit) than the traditional combination of split-ring resonators with wire strips, and one can identify a current trend to favor this kind of double-layer structure because it promises to achieve more efficient structures in terms of metamaterial properties, namely negative-refractive index, single-negative (SNG), and left-handed (LH) behavior over a certain frequency range [1]-[9]. Fishnet MTMs have been designed for microwave and optical frequency bands, mostly aiming at a single-band negative refractive index [1]-[6], [8] and less often for a multi-band negative index [7, 9]. In some cases, the structure does not provide negative permeability and the negative refractive index is achieved because of the existence of high losses [4, 7, 10, 11].

The exploitation of surface-plasmon-polaritons (SPPs) [12] has recently opened a novel approach for multi-band negative-index behavior [7, 9]. If the separation between the metallic layers of a fishnet structure is small enough, then SPPs are excited which yield several peaks in the transmission spectrum in addition to the main peak. These peaks create additional resonance modes and negative permeability can be achieved. However, it is known that the choice of metal is important for having higher-order resonance modes, but – according to the best of our knowledge – this aspect has not been studied well for THz fishnet MTMs. In this work, the effect of the metallization on the multi-resonance modes is discussed with regard to SNG/LH behavior at THz frequencies using numerical results.

2 Design and Analysis

In this section, the multi-band fishnet MTM will be introduced and then the metallization effect will be presented. The unit cell of the proposed multi-band fishnet MTM is shown in Figure 1. The dimensions of the structure have carefully been selected in order to enhance the higher-order modes. The structure can be considered as a combination of parallel metal plates along the magnetic-field direction, which provide the negative permeability, and pairs of continuous wires with modulated width along the electric-field direction which provide negative permittivity [9]. The metallization is initially assumed to be made of an ideal conductor (perfect electric conductor, PEC, whose conductivity σ was taken for practical reasons to be 1×10^{30} S/m in the simulations) and allows to achieve abrupt changes in the transmission owing to SPPs. Quartz glass with a thickness of 5 μm has been chosen as dielectric medium because of its moderate dielectric constant ($\epsilon_r = 3.75$) and low losses in the lower THz range (loss factor: less than 4×10^{-4}, dissipation factor: less than 1×10^{-4}, absorption coefficient: 10×10^{-6} cm^{-1}). The structure has been designed to have an identical configuration in the two lateral directions. Hence, the sample will operate equally for all polarizations, and the effective refractive index, as well as the effective permittivity and permeability, will be functionally independent of the polarization of the incident wave [9]. The simulations have been performed with a full-wave EM solver based on the finite integration

Received November 17, 2011; published March 22, 2012
ISSN 1990-2573

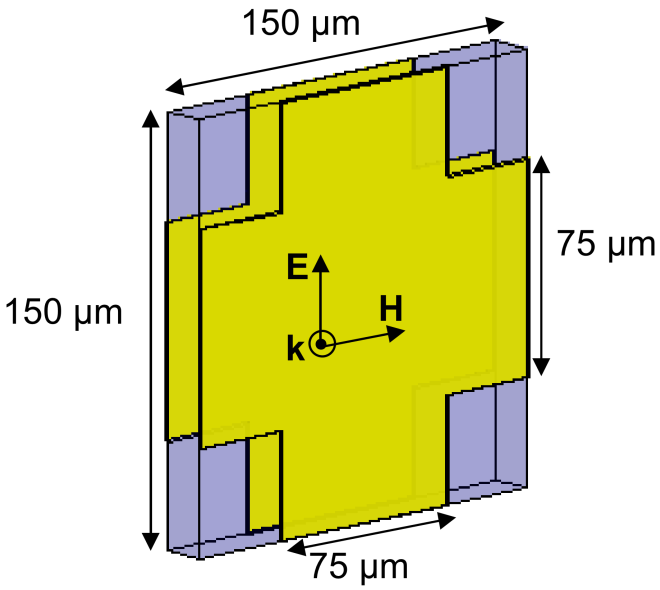

FIG. 1 The unit cell of the proposed THz fishnet MTM

Metal	f_p (THz)	γ (THz)
Ag	2180	4.35
Cu	1914	8.34
Au	2175	6.50
Al	3570	19.79
Pb	1781	35.22

TABLE 1 Plasma frequencies and damping rates of the investigated metals [15, 16]

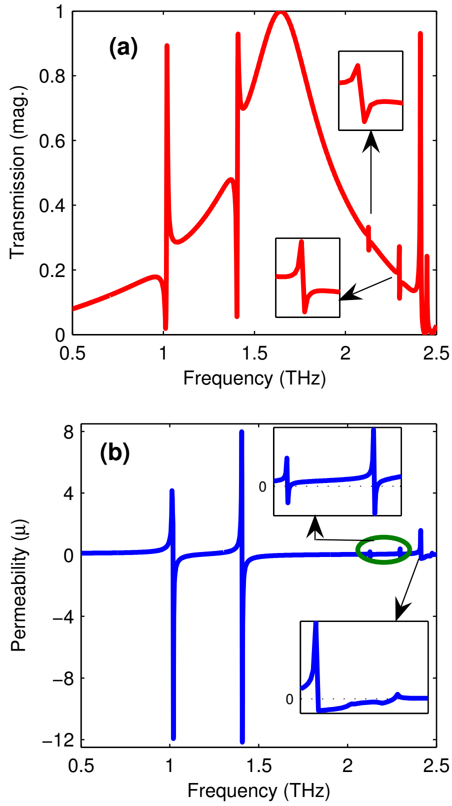

FIG. 2 The frequency dependence of the transmission (a) and of the real part of the effective permeability (b) for the THz fishnet MTM based on an ideal conductor

technique employing periodic boundary conditions along the lateral directions. Waveguide ports have been assumed for the excitations and detection of the THz wave. We have extracted the effective permeability by means of the standard retrieval methods [13, 14]. The Drude model approximation has been used to describe the effective dielectric properties of the different metals. The dielectric function can be written as $\epsilon(f) = 1 - f_p^2/\left(if\gamma + f^2\right)$, where f_p is the plasma frequency and γ the damping rate of the materials electrons [15, 16]. The values used for the plasma frequency and damping rate are given in Table 1.

Numerical results for the optimized fishnet MTM are shown in Figure 2. The thickness of the metallization is kept the same for all cases (both the PEC and the other metals) presented throughout this study. The transmission curve exhibits three pronounced and sharp changes because of the SPPs response, namely at around 1.0 THz, 1.4 THz and 2.4 THz, and a smaller sharp changes above 2.0 THz (see Figure 2(a)). A broad peak reaching unity value at around 1.65 THz dominates the transmission curve. It arises from the coupling of the incident wave to SPPs which leads to enhanced transmission (extra-ordinary transmission - EOT). However, the structure does not provide a magnetic resonance where the transmission has unity value, as can be observed from the frequency response of the permeability (Figure 2(b)). In this case, EOT occurs at the electric plasma frequency which sits at 1.65 THz and results from the field resonance of the wire array (effective plasma resonance). In addition, the effective impedance is perfectly matched to vacuum at 1.65 THz which explains the occurrence of the EOT. The derivative-like changes in the transmission can be attributed to magnetic resonances where the effective permeability is negative. The magnetic nature of the resonances is proven by the anti-symmetric response of the electric current distributions on the metallic parts of the structure (data not shown) [8, 9]. The magnetic resonance located at 2.4 THz is characterized by a less pronounced permeability change than that of the first two magnetic resonances (1.0 THz and 1.4 THz), but we still have a negative permeability at this frequency band. Furthermore, the first two resonances have LH character since the effective permittivity has two small anti-resonances at the locations of the first and second magnetic resonances which yields two spectral regions with negative refractive index [8, 9]. The other ones do not have LH character since the Drude-like permittivity is negative only below the plasma frequency at 1.65 THz, and hence the negative region only covers the first two magnetic resonances but not the others.

As a result, single-layer fishnet MTM slabs with suitable geometrical design parameters allow to obtain higher-order modes with strong resonances and with either LH or SNG character. Note that the higher-order modes (mostly dual-band) reported in the literature were mostly achieved using multi-layer MTM designs. Here, we achieve the higher-order resonances with only one slab and they number more than two in our case.

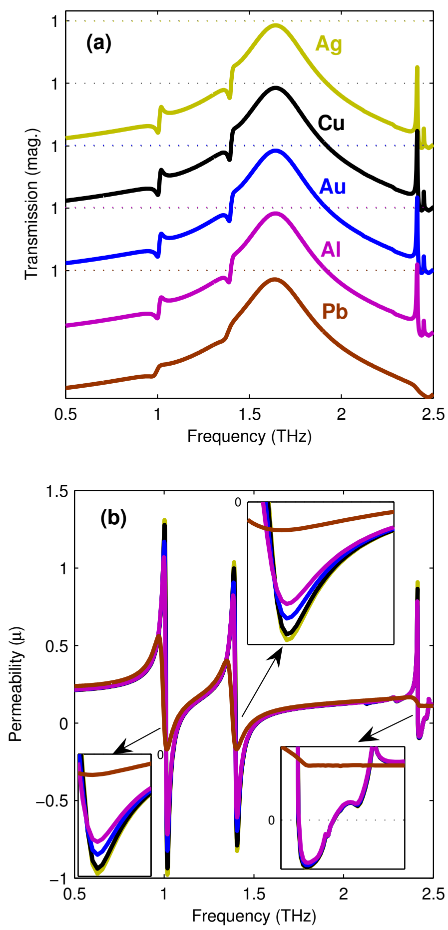

FIG. 3 Simulated transmission spectra (a) and the real part of the effective permeabilities (b) of the THz fishnet MTM for different metals. The curves are order in the sequence of the conductivity values (highest conductivity: Ag, lowest: Pb). The scale of the y-axis in Figure 3(a) is the same as in Figure 2(a).

We now address the choice of metal for the fabrication of the MTM. This choice carries major importance because it determines how well one can couple to the SPP modes and whether the excitation is strong enough to achieve the negative permeability needed for negative refraction. Figure 3 presents the frequency response of the transmission magnitude calculated for five metals. The scale of the transmission for each metal is the same as in Figure 2. The magnitude and shape of the resonances are affected by the change of the metallization, while the influence on their spectral positions remains so weak that we cannot discern shifts in the spectral positions of the resonances. We have verified that the current distributions on the metallic structures exhibit an anti-symmetric response at the resonance frequencies, thus corroborating the magnetic character of the resonances. EOT does not reach 100 % any more as for the ideal conductor, but we still have pronounced transmission for each metallization. The best EOT performance is observed for Ag and the worst for Pb. In comparison with the ideal conductor, the effective impedances do not matched perfectly with that of the vacuum any more, which is related with a reduced lifetime of the SPPs resulting from the non-vanishing damping rates.

With regard to the strength of the magnetic resonances, we can group the five data sets into two subsets, those of the good conductors Ag ($\sigma = 6.1\times10^7$ S/m), Cu ($\sigma = 5.8\times10^7$ S/m), Au ($\sigma = 4.1\times10^7$ S/m) and Al ($\sigma = 3.8\times10^7$ S/m) on one hand, and that of Pb ($\sigma = 5\times10^6$ S/m) as not quite such a good conductor on the other. For the first subset, we find that the three magnetic resonances (at around 1.0 THz, 1.4 THz, and 2.4 THz) are clearly less pronounced than in the EOT case, but all three of them are well discernible. The weakening of the features roughly scales with the reduction of the conductivity. For Pb, however, a more drastic change is found. The transmission curve exhibits the three resonances only weakly as step-like features; in fact, the third resonance has nearly vanished. In the permeability spectrum, the weakening of the third resonance is even more radical. While the first two resonances remain clearly visible, the third one, at 2.4 THz, has disappeared from the linear plot of the spectrum (it is still identifiable on a logarithmic representation of the data).

This extra-ordinarily strong weakening of the third resonance appears to be associated with the loss of the negative permeability. Among the three magnetic resonances discussed here for all metals, the third is the one which exhibits the weakest diamagnetic behavior. With decreasing conductivity, the third resonance loses its diamagnetic character earlier than the other resonances at some threshold value of the conductivity, and becomes paramagnetic. Ag, Cu, Au, and Al have conductivities above this threshold, while the conductivity of Pb is below. With the change of the character of the magnetic response, apparently the coupling strength of the electromagnetic wave to the resonance strongly decreases. The practical consequence is that the third resonance cannot be used for the design of MTM functionalities any more. Note that the magnetic resonances located above 2.0 THz and below 2.4 THz are completely vanishes in the case of the real metals with respect to PEC case.

3 Conclusion

We have presented a metallic fishnet metamaterial design which exhibits interesting properties in the THz spectral region such as (i) perfect-impedance matching to vacuum at a certain frequency which results in an extra-ordinarily strong transmission, (ii) strong multiband resonant character, and (iii) negative permeability and permittivity such that it is possible to have a negative refractive index in several spectral bands. We have investigated the effect of the metals conductivity on the transmission characteristics. It is observed that the type of metal used affects the transmission characteristics beyond the expected behavior which is that a reduction of the conductivity entails a corresponding weakening and smearing out of electromagnetic resonances. For a higher-order magnetic resonance, we find a more drastic and abrupt change which results in a near-suppression of the resonance if the conductivity of the metal falls below a certain threshold value. It appears that this abrupt weakening of the resonance is associated with the change of its magnetic response from diamagnetic to paramagnetic which then weakens the coupling of the electromagnetic wave to this resonance.

References

[1] G. Dolling, C. Enkrich, M. Wegener, J. F. Zhou, C. M. Soukoulis, and S. Linden, “Cut-wire pairs and plate pairs as magnetic atoms for optical metamaterials,” Opt. Lett. **30**, 3198–3200 (2005).

[2] S. Zhang, W. Fan, K. J. Malloy, and S. R. J. Brueck, “Near-infrared double negative metamaterials,” Opt. Express **13**, 4922 (2005).

[3] S. Zhang, W. Fan, N. C. Panoiu, K. J. Malloy, R. M. Osgood, and S. R. J. Brueck, “Experimental demonstration of near-infrared negative-index metamaterials,” Phys. Rev. Lett. **95**, 137404 (2005).

[4] U. K. Chettiar, A. V. Kildishev, H.-K. Yuan, W. Cai, S. Xiao, V. P. Drachev, and V. M. Shalaev, “Dual-band negative index metamaterial: double negative at 813 nm and single negative at 772 nm,” Opt. Lett. **32**, 1671–1673 (2007).

[5] M. Kafesaki, I. Tsiapa, N. Katsarakis, Th. Koschny, C. M. Soukoulis, and E. N. Economou, “Left-handed metamaterials: The fishnet structure and its variations,” Phys. Rev. B **75**, 235114 (2007).

[6] K. B. Alici, and E. Ozbay, “Characterization and tilted response of a fishnet metamaterial operating at 100 GHz,” J. Phys. D Appl. Phys. **41**, 135011 (2008).

[7] C. Garcia-Meca, R. Ortuno, F. J. Rodriguez-Fortuno, J. Marti, and A. Martinez, “Double-negative polarization-independent fishnet metamaterial in the visible spectrum,” Opt. Lett. **34**, 1603–1605 (2009).

[8] C. Sabah, and H. G. Roskos, “Numerical and experimental investigation of fishnet-based metamaterial in a X-band waveguide,” J. Phys. D Appl. Phys. **44**, 255101 (2011).

[9] C. Sabah, and H. G. Roskos, “Dual-band polarization-independent sub-terahertz fishnet metamaterial,” Curr. Appl. Phys. **12**, 443–450 (2012).

[10] M. W. McCall, A. Lakhtakia, and W. S. Weiglhofer, “The negative index of refraction demystified,” Eur. J. Phys. **23**, 353–359 (2002).

[11] R. A. Depine, and A. Lakhtakia, “A new condition to identify isotropic dielectric-magnetic materials displaying negative phase velocity,” Microw. Opt. Techn. Let. **41**, 315–316 (2004).

[12] C. Sabah, M. D. Thomson, F. Meng, S. Tzanova, and H. G. Roskos, “Terahertz propagation properties of free-standing woven-steel-mesh metamaterials: Pass-bands and signatures of abnormal group velocities,” J. Appl. Phys. **110**, 064902 (2011).

[13] A. M. Nicolson, and G. Ross, “Measurement of the intrinsic properties of materials by time domain techniques,” IEEE T. Instrum. Meas. **IM-19**, 377–382 (1970).

[14] W. B. Weir, “Automatic measurement of complex dielectric constant and permeability at microwave frequencies,” Proc. IEEE **62**, 33–36 (1974).

[15] P. B. Johnson, and R. W. Christy, “Optical constants of the noble metals,” Phys. Rev. B **6**, 4370–4379 (1972).

[16] M. A. Ordal, L. L. Long, R. J. Bell, S. E. Bell, R. R. Bell, R. W. Alexander, Jr., and C. A. Ward, “Optical properties of the metals Al, Co, Cu, Au, Fe, Pb, Ni, Pd, Pt, Ag, Ti, and W in the infrared and far infrared,” Appl. Optics **22**, 1099–1119 (1983).